Driving forces of global wildfires over the past millennium and the forthcoming century

O. Pechony[1] and D. T. Shindell

National Aeronautics and Space Administration (NASA) Goddard Institute for Space Studies and Columbia University, 2880 Broadway, New York, NY 10025

Edited by F. Stuart Chapin, University of Alaska, Fairbanks, AK, and approved September 10, 2010 (received for review March 19, 2010)

Recent bursts in the incidence of large wildfires worldwide have raised concerns about the influence climate change and humans might have on future fire activity. Comparatively little is known, however, about the relative importance of these factors in shaping global fire history. Here we use fire and climate modeling, combined with land cover and population estimates, to gain a better understanding of the forces driving global fire trends. Our model successfully reproduces global fire activity record over the last millennium and reveals distinct regimes in global fire behavior. We find that during the preindustrial period, the global fire regime was strongly driven by precipitation (rather than temperature), shifting to an anthropogenic-driven regime with the Industrial Revolution. Our future projections indicate an impending shift to a temperature-driven global fire regime in the 21st century, creating an unprecedentedly fire-prone environment. These results suggest a possibility that in the future climate will play a considerably stronger role in driving global fire trends, outweighing direct human influence on fire (both ignition and suppression), a reversal from the situation during the last two centuries.

biomass burning | fire modeling | human–environment interactions | paleoclimate

Once viewed as local phenomena, fires are now recognized as a global scale environmental process that has influenced the atmosphere and biosphere for hundreds of millions of years (1, 2). Today fires continue to directly influence human society and affect global climate. With a recent rise in the incidence of large uncontrolled fires, occurring regardless of national firefighting capacities (1, 3–7), concerns have grown about how climate change and human activities might impact future fire regimes. However, it is still unsettled whether climate or direct anthropogenic influence (fire ignition and suppression) are more important in determining global fire trends (1).

Recently we have developed a fire representation method for global climate models (8). We utilize it here for an attempt to reproduce past millennium fire activity trends and separate climatic and anthropogenic effects. The method estimates fire activity based on vegetation density, ambient meteorological conditions (temperature, relative humidity, and precipitation), availability of ignition sources (lightning and anthropogenic), and fire suppression rates. We base our historical estimates on simulations of 850–2003 CE (common era) climate conditions using the AR4 version of the Goddard Institute for Space Studies (GISS) general circulation model (GCM) (9, 10), and land-use and population density reconstructions from the History Database of the Global Environment (HYDE) 3.1 (11). The simulated climate variations and land-use changes are used to estimate baseline fire activity trends [assuming ubiquitous ignition source distribution (8)] without any direct human interference. Population densities are used to assess direct anthropogenic effects (fire ignition and suppression, both increasing with population density), assuming fire suppression effectiveness to increase with time. *Materials and Methods* and *SI Text* provide further details on the simulations setup.

Results

Past Fire Activity. Model results successfully recreate global fire activity variations reconstructed from sedimentary charcoal records (12) (Fig. 1*A*). Until the late 18th century, simulations either with or without direct anthropogenic influence agree well with reconstructed data, suggesting that during this period global fire activity was primarily climate-driven, whereas human influence remained relatively small. Although this is in general agreement with the charcoal data interpretation (12), we find that changes in global precipitation, rather than temperature, played a major role in determining global fire activity variations in the preindustrial period (*SI Text*). For instance, the cold and dry climate during the late 15th century Spörer Minimum (Fig. 1*B*) corresponds with increased global fire activity (in both the model-based and the charcoal-based reconstruction), whereas during the cold but humid Maunder Minimum (17th–early 18th centuries) global fire activity decreased. In the same epoch, sharp native population declines in both the Americas, following the European conquest, led to a decreased number of human-induced (but not “natural”) fires on these continents. However, because the overall anthropogenic influence on global fires was weak then, the estimated global effect of these changes was relatively small (Fig. 1*A*).

Following the Industrial Revolution (late 18th–early 19th centuries), human population expanded rapidly (Fig. 1*C*). Unprecedented rates of fossil fuel burning led to the onset of global warming (Fig. 1*B*). Over the 19th century both the model- and the charcoal-based records show sharp increases in biomass burning (Fig. 1*A*). Although changing climate and increasing population both contributed to this rise, model results suggest a stronger influence from direct anthropogenic activities, which in the 19th century became the dominant driver of global fire activity trends (*SI Text*). Expanding human population induced rapid land-use changes. Forests were cleared for agricultural land and pastures, reducing vegetation density (Fig. 1*C*), and hence the fuel amounts, slowing fire activity’s long-term rise. However, the common tool for land clearing was fire (13–16). Wildfire mapping for the 1880 US census, for instance, revealed staggering amounts of burning, predominantly of agricultural origins (15). Hence the land-clearing process itself could have boosted the number of fires in the early Industrial Period, contributing to the earlier increase of fire activity in the charcoal-based record. Extensive information on the worldwide history of land-clearing fires (which are currently not depicted in our model) is necessary to credibly assess their effect on global fire activity variations. Methane fire emissions reconstructed from Antarctic ice-core

ENVIRONMENTAL SCIENCES

Author contributions: O.P. and D.T.S. designed research; O.P. performed research; and O.P. and D.T.S. wrote the paper.

The authors declare no conflict of interest.

This article is a PNAS Direct Submission.

Freely available online through the PNAS open access option.

[1]To whom correspondence may be addressed. E-mail: opechony@giss.nasa.gov or pechony@gmail.com.

This article contains supporting information online at www.pnas.org/lookup/suppl/doi:10.1073/pnas.1003669107/-/DCSupplemental.

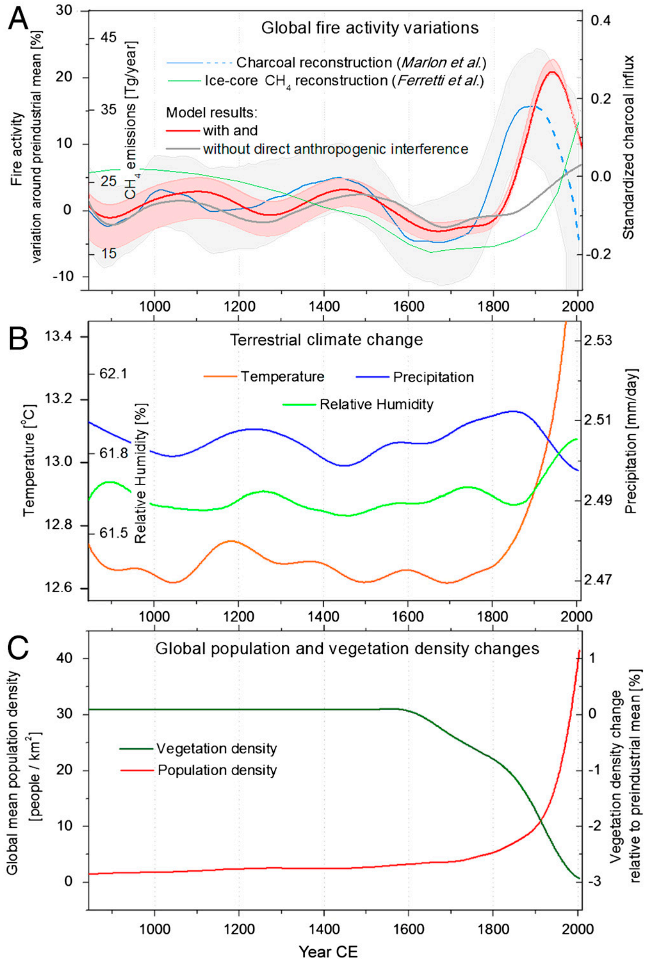

Fig. 1. Global fire activity, climate, vegetation, and population. (*A*) Modeled global fire activity variations (*SI Text*) with (red line) and without (gray line) direct anthropogenic influence (ignition and suppression): Red-shaded area represents uncertainty in the anthropogenic effect assumptions (*SI Text*); ice-core methane fire emissions reconstruction (green line) (17) and charcoal-based global fires reconstruction (blue line) with gray-shaded confidence interval (12) and blue dashed line indicating increased uncertainty in the late 20th century reconstructions. (*B*) GISS GCM annual means of the terrestrial area surface temperature (orange line), precipitation (blue line), and relative humidity (green line). (*C*) Global mean population (red line) and vegetation (green line) densities (11).

records (17) suggest a later fire activity increase (Fig. 1*A*). Although some skepticism exists as to whether this trend reflects fire emissions (18), differences between the ice-core and the charcoal-based reconstructions illustrate uncertainties in past fire activity (though different smoothing procedures could enhance differences between these datasets).

Around 1900 there is a sharp downturn in global fire activity, both in the model- and the charcoal-based records, despite increasing temperatures and decreasing precipitation. In accord with the charcoal-based interpretations (12), this downturn results from increasing fire suppression (accompanying population growth), and decreased vegetation density, but with stronger influence from direct anthropogenic activity (*SI Text*). Toward the late 20th century, the charcoal-based records' uncertainty increases, and they do not depict, for instance, increased burning in the tropics and the western United States in the past three decades (12). Although ice-core reconstructions show an increasing trend throughout the 20th century, it is likely that the downturn in the charcoal-based data, reproduced by the model both on a global scale and at the charcoal sites (*SI Text*), is real, though late 20th

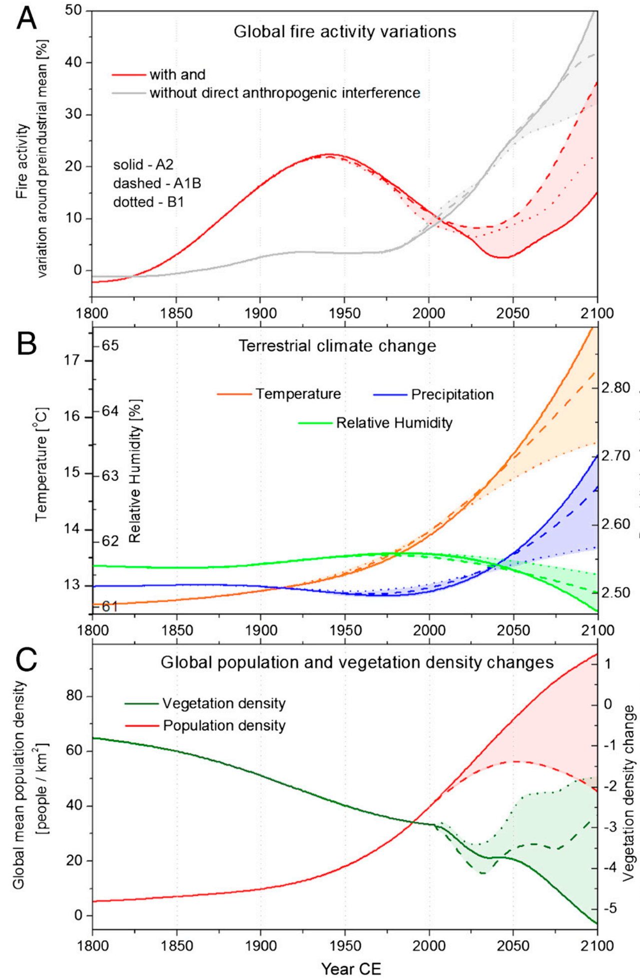

Fig. 2. Projected global fire activity, climate, vegetation, and population. Three SRES scenarios are shown: A2 ("maximum," continuing past variations with solid line), A1B ("midrange," dashed line), and B1 ("minimum," dotted line). (*A*) Modeled global fire activity with (red lines) and without (gray lines) direct anthropogenic interference; (*B*) GISS GCM annual means of the terrestrial surface temperature (orange lines), precipitation (blue lines), and relative humidity (green lines). (*C*) Global mean vegetation (green lines) and population (red lines) densities (A1B and B1 population scenarios coincide) (21).

century fire activity may be higher than implied by the charcoal-based records.

Future Fires. Overall, the model captures historical trends influenced by a variety of natural and anthropogenic factors remarkably well, inspiring some confidence in the model's projection of future fires. GISS GCM climate simulations (19), like other models, predict a significant warming over the forthcoming century (Fig. 2*B*). Rapidly rising temperatures and regional drying reverse the recent fire activity decline, driving a rapid increase after ~2050 in all three scenarios examined here, described in the Intergovernmental Panel on Climate Change Special Report on Emissions Scenarios (SRES) (20, 21) (Fig. 2*A* and *SI Text*). Population growth, and to a lesser extent, land-cover change (Fig. 2*C*), reduces the increase in fire activity, but does not reverse the long-term trend, even in the A2 scenario where anthropogenic pressure is strongest and continues to increase throughout the simulations. Ironically the more "optimistic" A1B and B1 scenarios that produce milder warming result in greater biomass burning due to reversal of land conversion and declining population (and hence fire suppression).

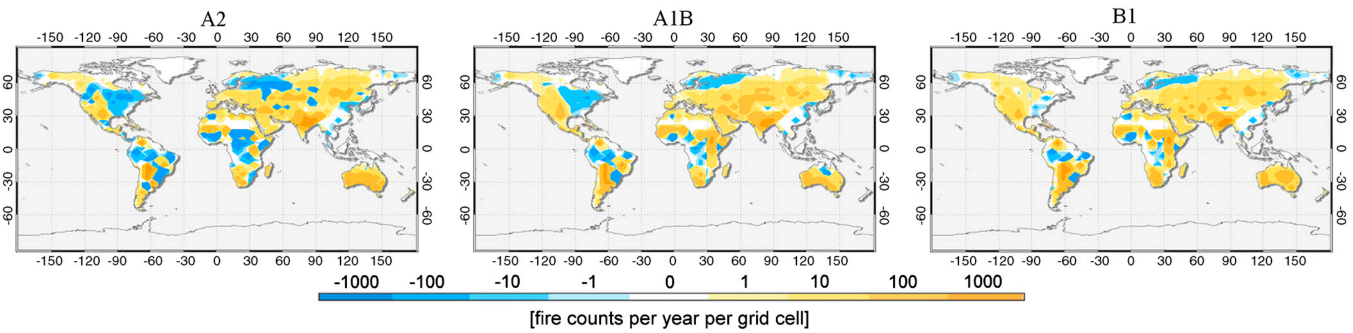

Fig. 3. Regional patterns of projected fire activity changes. Yellow shades indicate increases, and blue shades indicate decreases in linearized regional fire activity trends over the 21st century (years 2004–2100) in A2, A1B, and B1 scenarios.

Although global fire activity is projected to increase, this trend is not uniform worldwide. The broad spatial patterns of biomass burning trends are quite consistent across the scenarios (Fig. 3) and largely agree with another estimate (22). Less agreement is found with projections based on statistical relations between present-day climate and fires (23), which may be of limited value when applied to future climate due to shifting fire regime. Changes in the hydrologic cycle [some of which are robust features of climate models (24, *SI Text*)] play a large role in these projected regional variations, especially because temperatures rise nearly everywhere. Biomass burning trends in the United States (Fig. 4*A*) are a good example of the strong regional influence of hydrologic cycle changes. Although temperatures rise throughout the country, it becomes more humid and rainy in the East and drier in the West (Fig. 4*B*). Consequently, in the eastern United States fire activity declines, while rising considerably in the western United States (Fig. 4*A*). In both cases increasing population densities and land-cover changes (Fig. 4*C*) generally reduce fire activity. Our modeled 20th century eastern and western US trends agree fairly well with historical trends reconstructed for these regions by Mouillot and Field (25) (Fig. 4*A*). An exception is the first two decades of the century in the western United States, where the historical reconstruction shows increased burning, whereas our model indicates decreased fire activity. Although the historical reconstruction relies on data that are often too inconclusive to support consistent quantitative accuracy (25), it is likely that fire activity in the early 20th century was indeed higher throughout the United States, due to extensive agricultural fires (15, 25), which are not depicted by our model. However, the overall correspondence between reconstructed and modeled past fire trends provides reasonable confidence in our future regional estimates in areas where precipitation projections are relatively robust [such as North America, Europe, and Australia (24)]. Nevertheless, it should be emphasized that although our projections agree with some regional studies (4, 26–28), they disagree with others (29), highlighting the uncertainty associated with estimating the future influence of climate and humans on biomass burning. We also cannot negate the possibility that future technological or methodological advancements will drastically improve fire suppression effectiveness, allowing reduction of fire activity to significantly lower levels.

Discussion

Although we have obtained quite reasonable agreement with reconstructed fire histories, our estimates of anthropogenic effects on global fires rely on highly incomplete information on fire-related human activities. Not only historical, but also comprehensive contemporary global data on anthropogenic ignitions and fire suppression are currently lacking. There is a need for comprehensive knowledge of worldwide anthropogenic fire management history, especially in the Industrial Period, to better resolve the role of humans in past fire activity, and more reliably assess their impact on future biomass burning. Nonetheless, these results present a major advance in biomass burning representation in climate models, reproducing the reconstructed millennium-long fire history. Our results indicate a precipitation-driven preindustrial fire regime, shifting to an anthropogenic-driven regime in the 18th century, and an imminent shift to a temperature-driven global fire regime in the future. This suggests a real possibility that fire management policies will have to adapt to a world in which climate plays a substantially stronger role in driving fire trends,

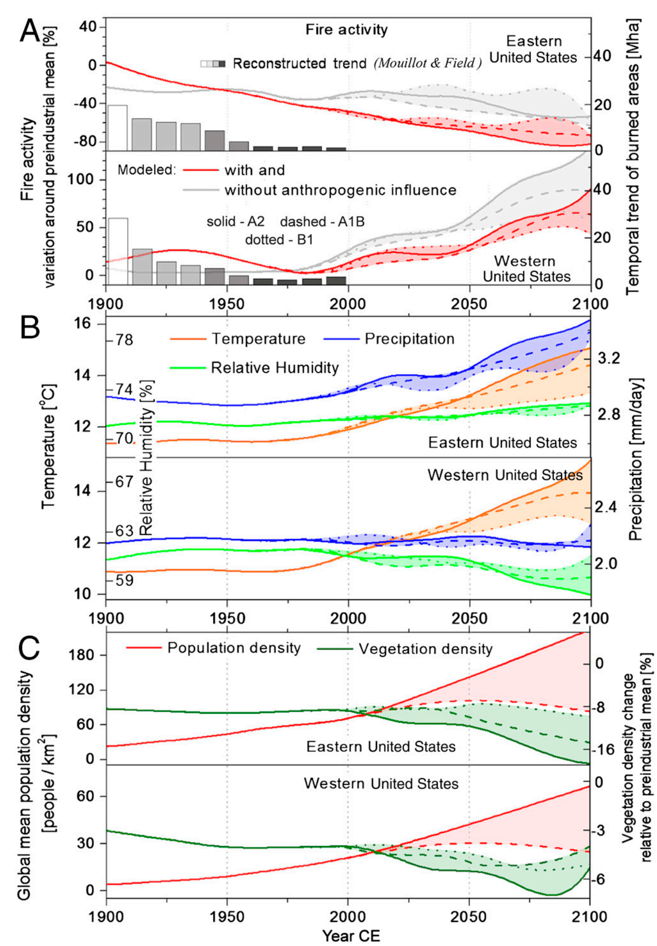

Fig. 4. Past and future fire activity, climate, vegetation, and population in the United States. Quantities are the same as in Fig. 2, but each plot shows two regions: the eastern (upper plots) and western (lower plots) United States. Bars show decadal reconstructions of temporal trends of burned areas for the two regions (25), which can be qualitatively compared with fire activity. Bar color indicates reconstruction reliability (25)—"accurate" (black), "good" (gray), "poor" (light gray), and "very poor" (white).

outweighing direct human influence on fire, a reversal from the situation during the last two centuries.

Materials and Methods

Fire activity estimates (see ref. 8 for detailed method description and evaluation) are based on temperature, precipitation, relative humidity, and lightning activity generated in AR4 GISS GCM climate simulations and HYDE (past) and Integrated Model to Assess the Global Environment (IMAGE) (future) land-cover and population density datasets. Climate during the 844–1880 CE simulations (9) was driven by variations in solar irradiance [responsible for the vast majority of multidecadal time-scale forced variability (30)]; 1880–2003 simulations (10) were driven by multiple forcings, including greenhouse gases, tropospheric aerosols, ozone, solar irradiance, and volcanic aerosols; 2004–2100 simulations (19) were driven by changes in the well-mixed greenhouse gases [the dominant climate forcing over the past few decades (19)]. Anthropogenic ignition sources are calculated as an increasing function of population density while assuming that people living in sparsely populated regions interact more with natural ecosystems and therefore produce potentially more ignitions (31). Fire suppression rates also increase with population density (8), with suppression rates kept constant at present-day level in regions with high population density (occurring relatively recently), whereas in the unpopulated areas no fire suppression is assumed at the beginning of the simulations, increasing to present-day levels by the 21st century, and remaining constant thereafter. Two alternative scenarios were calculated to characterize the uncertainty associated with our assumptions on past fire suppression rates (defining the boundaries of the red-shaded area in Fig. 1*A*); however, the general behavior of the global fire activity trends remained similar. *SI Text* provides further discussion of the setup of the simulations and the uncertainty associated with our assumptions on fire suppression rates, the contribution of individual model parameters to the fire activity trend, global fire activity variations vs. variations at the charcoal sites, zonal fire activity trends, and the data smoothing procedure.

ACKNOWLEDGMENTS. We sincerely thank Dr. Jennifer Marlon (University of Oregon, Eugene, OR) for sharing with us the charcoal-based reconstruction data. We thank the satellite data teams that created global fire analyses enabling quantitative evaluation of global fire models, and NASA's Modeling and Analysis Program and Applied Sciences Program for supporting this work.

1. Bowman DM, et al. (2009) Fire in the Earth system. *Science* 324:481–484.
2. Scott AC, Glasspool IJ (2006) The diversification of Paleozoic fire systems and fluctuations in atmospheric oxygen concentration. *Proc Natl Acad Sci USA* 103:10861–10865.
3. Pyne SJ (2001) *Fire: A Brief History* (Univ of Washington Press, Seattle).
4. Westerling AL, Hidalgo HG, Cayan DR, Swetnam TW (2006) Warming and earlier spring increase western U.S. forest wildfire activity. *Science* 313:940–943.
5. Lohman DJ, Bickford D, Sodhi NS (2007) Environment: The burning issue. *Science* 316:376.
6. Page SE, et al. (2002) The amount of carbon released from peat and forest fires in Indonesia during 1997. *Nature* 420:61–65.
7. Forsyth GG, van Wilgen BW (2008) The recent fire history of the Table Mountain National Park and implications for fire management. *Koedoe* 50:3–9.
8. Pechony O, Shindell DT (2009) Fire parameterization on a global scale. *J Geophys Res* 114:D16115 10.1029/2009JD011927.
9. Mann ME, et al. (2009) Global signatures of the Little Ice Age and Medieval Climate Anomaly and plausible dynamical origins. *Science* 326:1256–1260.
10. Hansen J, et al. (2007) Climate simulations for 1880–2003 with GISS modelE. *Clim Dynam* 29:661–696.
11. Goldewijk KK, van Drecht G (2006) HYDE 3: Current and historical population and land cover. *Integrated Modelling of Global Environmental Change. An Overview of IMAGE 2.4*, eds AF Bouwman, T Kram, and KK Goldewijk (PBL, Bilthoven, The Netherlands), pp 93–112.
12. Marlon JR, et al. (2008) Climate and human influences on global biomass burning over the past two millennia. *Nat Geosci* 1:697–702.
13. Arnold K, Burcham LT, Fenner RL, Grah RF (1951) Use of fire in land clearing. *Calif Agric* June 1951:13–15.
14. Hanks LM (1972) *Rice and Man: Agricultural Ecology in Southeast Asia* (Aldine Pub Co, Chicago).
15. Pyne SJ (1988) *Fire in America: A Cultural History of Wildland and Rural Fire* (Princeton Univ Press, Princeton).
16. Pyne SJ (1997) *Vestal Fire: An Environmental History, Told Through Fire, of Europe and Europe's Encounter with the World* (Univ of Washington Press, Seattle).
17. Ferretti DF, et al. (2005) Unexpected changes to the global methane budget over the past 2000 years. *Science* 309:1714–1717.
18. Houweling S, van der Werf G, Goldewijk KK, Röckmann T, Aben L (2008) Early anthropogenic emissions and the variation of CH_4 and $^{13}CH_4$ over the last millennium. *Global Biogeochem Cycles* 22:GB1002 10.1029/2007GB002961.
19. Hansen J, et al. (2007) Dangerous human-made interference with climate: A GISS modelE study. *Atmos Chem Phys* 7:2287–2312.
20. Nakicenovic N, Swart R (2000) *Special Report on Emissions Scenarios* (Cambridge Univ Press, Cambridge, UK).
21. RIVM (2001) The IMAGE 2.2 implementation of the SRES scenarios. (RIVM, Bilthoven, The Netherlands) CD_ROM publication 481508018.
22. Scholze M, Knorr W, Arnell NW, Prentice IC (2006) A climate-change risk analysis for world ecosystems. *Proc Natl Acad Sci USA* 103:13116–13120.
23. Krawchuk MA, Moritz MA, Parisien MA, Dorn JV, Hayhoe K (2009) Global pyrogeography: The current and future distribution of wildfire. *PLoS ONE* 4:e5102.
24. Meehl GA, et al. (2007) *Climate Change 2007: The Physical Science Basis*, eds S Solomon et al. (Cambridge Univ Press, Cambridge, UK), pp 748–845.
25. Mouillot F, Field CH (2005) Fire history and the global carbon budget: A $1° \times 1°$ fire history reconstruction for the 20th century. *Global Change Biol* 11:398–420.
26. Whitlock C, Shafer SL, Marlon J (2003) The role of climate and vegetation change in shaping past and future fire regimes in the northwestern US and the implications for ecosystem management. *Forest Ecol Manag* 178:5–21.
27. Brown TJ, Hall BL, Westerling AL (2004) The impact of twenty-first century climate change on wildland fire danger in the western United States: An applications perspective. *Climatic Change* 62:365–388.
28. Spracklen DV, et al. (2009) Impacts of climate change from 2000 to 2050 on wildfire activity and carbonaceous aerosol concentrations in the western United States. *J Geophys Res* 114:D20301 10.1029/2008JD010966.
29. Flannigan MD, Stocks BJ, Wotton BM (2000) Climate change and forest fires. *Sci Total Environ* 262:221–229.
30. Ammann CM, et al. (2007) Solar influence on climate during the past millennium: Results from transient simulations with the NCAR Climate System Model. *Proc Natl Acad Sci USA* 104:3713–3718.
31. Venevsky S, Thonicke K, Stich S, Cramer W (2002) Simulating fire regimes in human-dominated ecosystems: Iberian Peninsula case study. *Global Change Biol* 8:984–998.

Supporting Information

Pechony and Shindell 10.1073/pnas.1003669107

SI Text

Setup of the Simulations. ***Fire representation.*** A recently developed fire representation method for global climate models (1) provides a convenient and flexible tool for estimating global fire trends, while allowing separation of climatic and direct anthropogenic effects. The method is described in detail in Pechony and Shindell (1), thus here we will provide only a brief overview. Following principles of well-established methodologies in wide use by national land-management agencies (2–4), the algorithm estimates flammability based on vegetation density (i.e., fuel availability) and ambient meteorological conditions: temperature and relative humidity (that define the vapor pressure deficit), and precipitation (assuming an inverse exponential dependence of flammability on precipitation). The actual number of fires is then determined based on the availability of ignition sources—lightning and anthropogenic, and the expected effectiveness of fire suppression (assumed to increase exponentially with population density). Anthropogenic ignition sources are calculated as an increasing function of population density (5) while assuming that people living in sparsely populated regions interact more with natural ecosystems and therefore produce potentially more ignitions.

Extensive validation of the fire parameterization described above is documented in Pechony and Shindell (1). The method was shown to reproduce present-day spatial distributions and the seasonal variability of global fires in good correspondence with modern satellite observations by the Moderate Resolution Imaging Spectroradiometer and Visible and Infrared Scanner instruments. Two decades of data from the Advanced Very High Resolution Radiometer were used to validate modeled fire activity variations over the years 1980–2000, showing the ability of the model to adequately reproduce interannual fire activity variations, as well as depict the response of global fire activity to climate perturbations following large volcanic eruptions. Here we exploit this method for estimating trends of global wildfires from the year 844 to 2100 CE (common era).

Climate and vegetation. Our estimates are based on simulations of climate conditions over the past millennium using the AR4 (Intergovernmental Panel on Climate Change Fourth Assessment Report) version of the Goddard Institute for Space Studies (GISS) general circulation model (GCM). We use averages from an ensemble of six 844–1880 climate simulations (6) driven by variations in solar irradiance. Though the simulations do not include other historical forcings such as volcanism, solar forcing appears to be responsible for the vast majority of multidecadal time-scale forced variability (7). The GISS simulations capture changes seen in proxy-network reconstructions of land-area surface temperatures relatively well, especially in the extratropics, including the temperature fluctuations between the 15th–18th century Little Ice Age and the Medieval Climate Anomaly (6), though the overall amplitude of long-term variations tends to be on the low side of the reconstructed range. Land-use reconstructions for all historical times are taken from the History Database of the Global Environment (HYDE) version 3.1 dataset (8). Climate simulations over 1880 to 2003 were driven by multiple forcings, including greenhouse gases (GHGs), tropospheric aerosols, ozone, solar irradiance, and volcanic aerosols, with reasonable agreement between the GCM and the observed temperatures (9). Future climate simulations (10) are driven by changes in the well-mixed GHGs, which have become the dominant climate forcing over the past few decades (10). Future land-cover projections are taken from the Integrated Model to Assess the Global Environment (IMAGE) version 2.2 database (11) and include responses of vegetation cover to GHG forced climate change, as well as changes due to land use. (Dynamic response of vegetation to fires is not included in this study, and would become feasible with coupling of the GCM with a dynamic vegetation model.) Baseline fire activity trends are estimated from the simulated climate variations and land-use changes, assuming a ubiquitous ignition source distribution (1), without any direct human interference. Such trends conveniently reflect variations in the background flammability conditions that influence the global fire activity, while also reflecting the estimated situation in a "world without direct human-fire interactions," because the influence of lightning activity variations on the global fire trend is very small (Fig. S1).

The reconstructions we use for comparison with the modeled fire trends are all proxies of different parameters, each effectively reflecting the long-term fire activity trends; we use fire counts as an identifier of fire activity variations. It should be noted, however, that over the long time scales considered here, burned areas calculated from these fire counts using vegetation-weighting technique (1, 12) are highly correlated with fire counts (Fig. S2) (which is often not the case over time scales of several years), making the bicentennially smoothed trends of fire counts and burnt areas virtually indistinguishable.

Ignition sources and suppression effect. To assess direct anthropogenic effects (fire ignition and suppression), we rely on population density from the same HYDE and IMAGE datasets as used for vegetation/land use. GISS GCM cloud-to-ground lightning discharges are used as natural ignition sources. The 1880–2100 simulations did not include lightning; thus for this period we use the average lightning map from the last decade of the solar simulations. We assume that this introduces only negligible inaccuracy to the fire trends, because over the period of solar simulations the influence of variations in lightning activity on the global fire trend was very weak (Fig. S1). Boundary conditions for present-day fire suppression (which is applied to all fires) are set at the values that have been shown to reproduce the modern fire activity behavior (1): 95% of fires are assumed to be suppressed in the most densely populated areas (these suppression rates are approached when population exceeds ~100 persons/km^2), and 5% are suppressed in wild, unpopulated areas. Fire suppression becomes perceptible at densities of ~1 person/km^2. The resulting number of anthropogenic fires increases with population density, reaching a maximum at densities of ~10 persons/km^2 and then falls due to increasing fire suppression (1). Such behavior is generally consistent with present-day global fire records (1), but the exact parameters of fire suppression are rather uncertain and probably vary around the globe. Yet higher uncertainty exists in the historical values. Because of the lack of comprehensive global data (historical or contemporary), we make heuristic assumptions. We know that the history of organized firefighting and prevention dates back at least to ancient Rome (13), and probably earlier. Although firefighting effectiveness depends on technical and economical factors, in general the success of fire suppression is conditioned by early fire detection. We thus keep fire suppression boundary conditions constant in heavily populated regions (note that such dense settlements occur only relatively recently) and increase them linearly from 0% to the present-day value of 5% in wild, unpopulated areas. In the future simulations we assume fire suppression rates remain at present-day levels.

To characterize the uncertainty associated with our assumptions on past fire suppression rates, we calculate two alternative scenarios. One assumes identical conditions for the unpopulated areas (increasing from 0% to 5%), but in and near dense populations fire suppression rates rise linearly from 50% to present-day values of 95%. The other assumes present-day fire suppression levels through the entire simulation period both in human settlements and in the wild (95% and 5%, respectively). The latter case is probably the lowest estimate, as firefighting in the past could hardly have been more efficient than it is today. These two scenarios define the boundaries of the red-shaded area in Fig. 1*A* (main text), characterizing the uncertainty associated with our anthropogenic effect assumptions. In the first scenario (the upper boundary of the red-shaded area) fire suppression rates in densely populated regions decrease significantly as we go back in time, but this has little effect on the global fire activity trend, because the extent of dense settlements, where these changes are important, also decreases. In the second scenario (the lower boundary), changes in fire suppression rates seem less significant, but they influence the sparsely populated regions that were more abundant in the past and thus have a more pronounced effect on the global fire trend. However, the general behavior of the global fire activity trend remains similar in all scenarios considered here, corresponding reasonably to the trend reconstructed from the charcoal records (Fig. 1*A*, main text). Note that uncertainty in global mean climate sensitivity or in the input solar forcing would primarily affect the magnitude of the fire trends and not their temporal behavior. Uncertainties in the response of the hydrologic cycle to climate change are larger; however, the major large-scale features of the response (as noted in the main text and discussed in the next section) are robust across climate models (14).

Contribution of model parameters to the fire activity trend. To assess the contribution of each model parameter to the fire activity trend, we calculated fire activity variations allowing only one of the parameters to change with time, while keeping others constant at the year 844 values (Fig. S1). (Hence the variations are presented around year 844 values, not the preindustrial mean as in Figs. 1*A* and 2*A* in the main text.) The sum of the resulting individual contributions is quite close to the actual fire activity trends: to the baseline trend (without direct anthropogenic influence) when contributions from climate parameters and land-cover change are summed, and to the trend including anthropogenic influence, when summed altogether. These contributions thus reflect the role of individual model parameters in global fire trends quite well (though not completely, as they only show the global means).

During preindustrial times global fire activity variations were driven primarily by climate and were weakly influenced by the slowly increasing population; the land-use change contribution became perceptible after ~1700 (Fig. S1). Model results suggest that on a global scale, precipitation (rather than temperature) played a very important role during this period, accounting for ~70% of the global fire activity variations (Fig. S1). For example, the global temperature decrease during the Maunder Minimum was accompanied by rising precipitation and relative humidity (Fig. 1*B*, main text) and corresponds with globally decreased fire activity, whereas the previous cold but dry Sporer Minimum (in solar output ~1430–1470) corresponds with increased fire activity (in both the model- and the charcoal-based reconstruction). Examples of long-term fire activity trends controlled by wet/dry conditions rather than temperature were described in some regional studies (15–18), although on such small regional scales other factors may become increasingly important, such as local anthropogenic pressure or temperature and precipitation seasonality (e.g., ref. 18). [Over large spatial and temporal scales, GCM trends of annual and summer temperature and precipitation are broadly coherent (Fig. S4*c*).] Although GCM precipitation variations are relatively small during the preindustrial period (Fig. 1*B*, main text), precipitation influence on flammability is inverse exponential; thus the effects of these relatively small changes overwhelm the temperature contribution. Such strong dependence of flammability on precipitation is not specific to our model and is reflected in the well-established fire-risk assessment methodologies (2–4). The variations in historical temperature simulated by the GCM are of reasonable magnitude compared to reconstructed temperature histories (19), and thus unlikely to be greatly underestimated. In fact, it appears that global temperature changes of the magnitude projected for the future are required to overwhelm precipitation-induced fire activity variations (Fig. S1), and past millennium temperature reconstructions (20, 21) do not suggest such strong temperature variations.

In the industrial era, anthropogenic effect became the main driver of global fire activity (Fig. S1). Climate change accounts for ~20% of the 19th century rise in global burning with the rest contributed by direct anthropogenic interference (fire ignition) that also forces the 20th century downturn in the global fire activity (due to fire suppression). However, in the 21st century, climate (itself projected to be driven by human activities) reassumes its dominant role in global fire activity variations and forces a rapid increase in global fire activity after ~2050. This rise is caused primarily by rapidly increasing global temperatures (Fig. S1), accompanied by declining relative humidity and regional precipitation reductions (despite an increasing global mean). Although these hydrologic cycle changes are more model-dependent than surface temperature, decreases in precipitation in Southern Europe, North Africa, Central America, Southernmost Africa, and at least parts of Australia and the western United States, as well as precipitation increases in Northern Eurasia, are robust features of climate models (14). These large-scale patterns define much of the regional fire activity trends shown in Fig. 3 (in the main text) and are related to well-known phenomena in the climate system [e.g., the enhancement of the extant tropical-subtropical precipitation pattern (22) and the strengthening of the Northern Annular Mode (23)]. Our projections of regional trends largely agree with estimates made with higher resolution models (24), suggesting that despite its coarse resolution the GCM is able to capture the general large-scale regional trends and serve as a reasonable basis for long-term fire projections. Further research directions could include finer resolution modeling to allow capturing topographic effects on climate and better representing responses in neighboring areas with distinct ecosystems, elaboration of fire suppression representation to include dependence on socioeconomic and climatic conditions, and study of the lagged responses due to fuel amount changing.

Global fire trend vs. trend at the charcoal sites. Model simulations provide global results, whereas the charcoal-based reconstruction is based on data collected from hundreds of isolated sites (21). Marlon et al. (21) examined these sites in terms of geographic, climatic, and vegetation space distribution and found that the dataset could be considered a reasonable representation of global biomass burning. To ensure that the modeled global fire activity trend can be comprehensibly compared with the trend derived from the charcoal records, we conducted analyses using only pixels roughly overlapping with the charcoal sites (model resolution is $4° \times 5°$, whereas each charcoal site represents a much smaller area). These results (Fig. S3) suggest that fire activity variations at the charcoal sites reflect the global fire activity variations quite well, in agreement with the Marlon et al. (21) analysis.

Zonal fire activity trends. The strength of the charcoal-based reconstruction lies in good coverage of climatic zones and major biomes, which allows it to be considered a reasonable representation of global fire activity despite the limited number of charcoal sites (21). Zonal reconstructions are less confident, especially in the tropics and southern extratropics (Fig. S4*a*), where site coverage is considerably scarcer than in the northern extratropics (21). Nevertheless, these reconstructions demonstrate differences between fire activity trends in different zones, which are reasonably depicted by the model, especially in the extratropics, where GISS simulations best capture reconstructed climate variations over the last millennium (6). Similar to the global fire activity trends, the modeled zonal trends are driven primarily by precipitation during the preindustrial period (Fig. S4*b*).

On a global scale the model predicts a stark shift in the future fire activity behavior. Although preindustrial variations of global fire activity are highly influenced by precipitation (Figs. S1 and S5*a*), in the future temperature becomes the dominant factor [and because global fire activity increases despite increasing global precipitation, fires appear correlated with precipitation (instead of being anticorrelated)]. However, on a point-by-point basis (Fig. S5*b*), both temperature and precipitation are important: As we go to smaller scales, fire activity becomes a more sensitive interplay of temperature, precipitation, and other factors, and the regime shift is evident only at large scales.

Data smoothing. In this work all data were smoothed with a Savitzky–Golay (26) smoothing filter using a 200-y window [the same window size was used in the charcoal-based reconstructions (21)] and a third degree local polynomial regression. The main advantage of Savitzky–Golay smoothing is that it tends to preserve features of the data, such as peak height and width, and is capable of retaining the overall profile for large window sizes.

1. Pechony O, Shindell DT (2009) Fire parameterization on a global scale. *J Geophys Res* 114:D16115, 10.1029/2009JD011927.
2. Nesterov VG (1949) *Flammability of the Forest and Methods for Its Determination (Gorimost lesa i metodi eio opredelenia)* (Goslesbumizdat, USSR State Ind Press, Moscow) (in Russian).
3. Zhdanko VA (1965) Scientific basis of development of regional scales and their importance for forest fire management, *Contemporary Problems of Forest Protection from Fire and Firefighting*, edited by Melekhov IS (Lesnaya Promyshlennost, Moscow), pp 53–86 (in Russian).
4. Keetch JJ, Byram GM (1968) A drought index for forest fire control, Research Paper SE-38, Forest Service, Southeastern Forest Experiment Station, US Department of Agriculture, Asheville, NC.
5. Venevsky S, Thonicke K, Stich S, Cramer W (2002) Simulating fire regimes in human-dominated ecosystems: Iberian Peninsula case study. *Global Change Biol* 8:984–998.
6. Mann ME, et al. (2009) Global signatures of the Little Ice Age and Medieval Climate Anomaly and plausible dynamical origins. *Science* 326:1256–1260.
7. Ammann CM, et al. (2007) Solar influence on climate during the past millennium: Results from transient simulations with the NCAR Climate System Model. *Proc Natl Acad Sci USA* 104:3713–3718.
8. Goldewijk KK, van Drecht G (2006) HYDE 3: Current and historical population and land cover. *Integrated Modelling of Global Environmental Change. An Overview of IMAGE 2.4*, eds Bouwman AF, Kram T, Goldewijk KK (PBL, Bilthoven, The Netherlands), pp 93–112.
9. Hansen J, et al. (2007) Climate simulations for 1880–2003 with GISS modelE. *Clim Dynam* 29:661–696.
10. Hansen J, et al. (2007) Dangerous human-made interference with climate: A GISS modelE study. *Atmos Chem Phys* 7:2287–2312.
11. RIVM, (2001) The IMAGE 2.2 implementation of the SRES scenarios (RIVM, Bilthoven, The Netherlands), (CD_ROM publication 481508018).
12. Van der Werf GR, Randerson JT, Collatz GJ, Giglio L (2003) Carbon emissions from fires in tropical and subtropical ecosystems. *Global Change Biol* 9:547–562.
13. Hirst J (1884) *On the Methods Used by the Ancient Romans for Extinguishing Conflagrations* (Willam Polard, Exeter, UK).
14. Meehl GA, et al. (2007) Global Climate Projections. *Climate Change 2007: The Physical Science Basis*, eds Solomon S, et al. (Cambridge Univ Press, Cambridge, UK), pp 748–845.
15. Swain AM (1978) Environmental changes during the past 2000 years in north-central Wisconsin: Analysis of pollen, charcoal, and seeds from varved lake sediments. *Quaternary Res* 10:55–68.
16. Filion L (1984) A relationship between dunes, fire and climate recorded in the Holocene deposits of Quebec. *Nature* 309:543–546.
17. Filion L, Saint-Laurent D, Desponts M, Payette S (1991) The late Holocene record of aeolian and fire activity in northern Québec, Canada. *The Holocene* 1:201–208.
18. Carcaillet C, Richard PJH (2000) Holocene changes in seasonal precipitation highlighted by fire incidence in eastern Canada. *Clim Dynam* 16:549–559.
19. Mann ME, et al. (2009) Global signatures of the Little Ice Age and Medieval Climate Anomaly and plausible dynamical origins. *Science* 326:1256–1260.
20. Jansen E, et al. (2007) Palaeoclimate. *Climate Change 2007: The Physical Science Basis*, eds Solomon S., et al. (Cambridge Univ Press, Cambridge, UK 2007), pp 433–497.
21. Marlon JR, et al. (2008) Climate and human influences on global biomass burning over the past two millennia. *Nat Geosci* 1:697–702.
22. Held IM, Soden BJ (2006) Robust responses of the hydrological cycle to global warming. *J Climate* 19:5686–5699.
23. Miller RL, Schmidt GA, Shindell DT (2006) Forced annular variations in the 20th century Intergovernmental Panel on Climate Change Fourth Assessment Report models. *J Geophys Res* 111:D18101, 10.1029/2005JD006323.
24. Scholze M, Knorr W, Arnell NW, Prentice IC (2006) A climate-change risk analysis for world ecosystems. *Proc Natl Acad Sci USA* 103:13116–13120.
25. Nakicenovic N, Swart R (2000) *Special Report on Emissions Scenarios* (Cambridge Univ Press, Cambridge, UK).
26. Savitzky A, Golay MJE (1964) Smoothing and differentiation of data by simplified least squares procedures. *Anal Chem* 36:1627–1639.

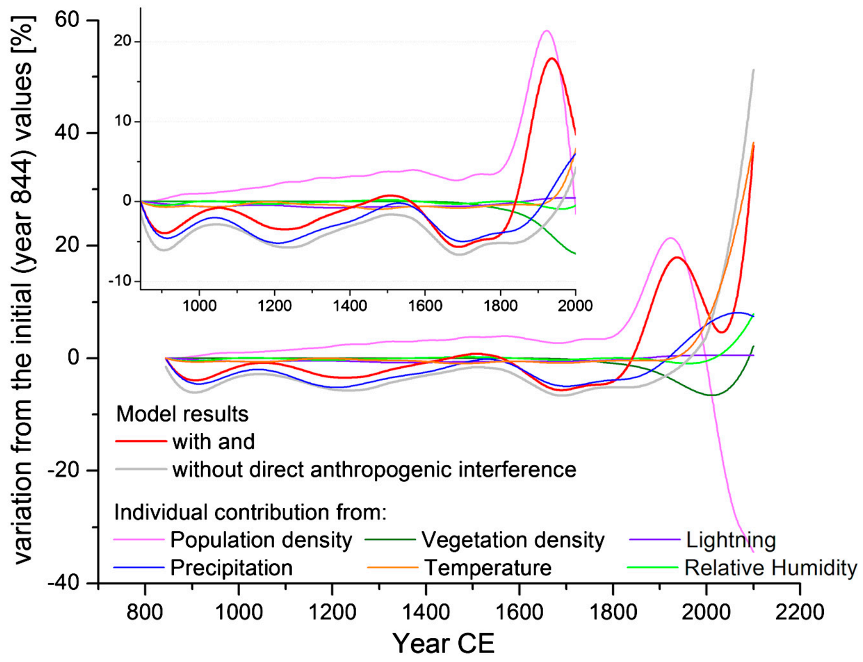

Fig. S1. Contribution of individual parameters to the global fire trend. Modeled fire activity trends with (red line) and without (gray line) direct anthropogenic influence, and the contribution of each model parameter to these trends: population (magenta line) and vegetation (olive green line) densities, precipitation (blue line), temperature (orange line), relative humidity (green line), and lightning activity (violet line; this contribution is very small). Variations after year 2003 were calculated for the A1B scenario of the Special Report on Emissions Scenarios (SRES) (25).

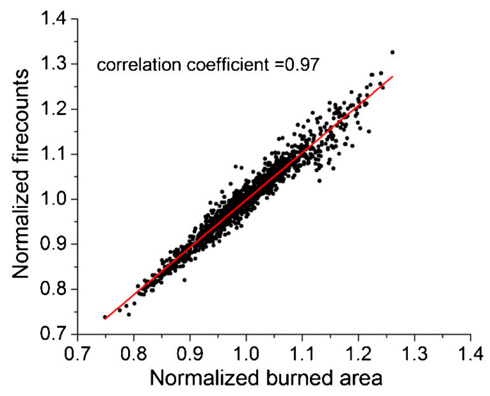

Fig. S2. Modeled global annual mean fire counts and burnt areas for each year during 844–2000 CE, normalized by the long-term mean. (No smoothing was applied to the datasets.)

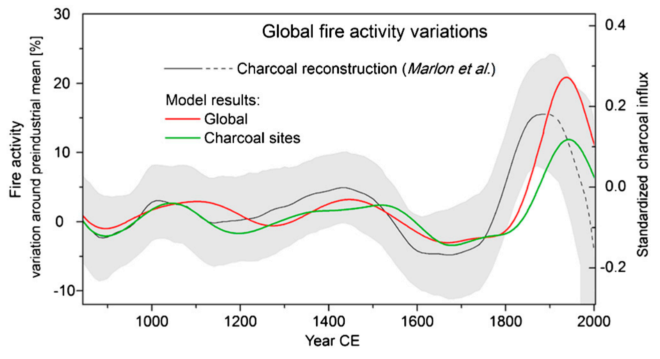

Fig. S3. Global results vs. results at the charcoal sites. Modeled variations of the global fire activity (red line) and fire activity at the charcoal sites (green line), and charcoal-based reconstruction of global fires (black line) with gray-shaded confidence interval (21). (The black dashed line indicates the increased uncertainty in the twentieth century charcoal reconstructions.)

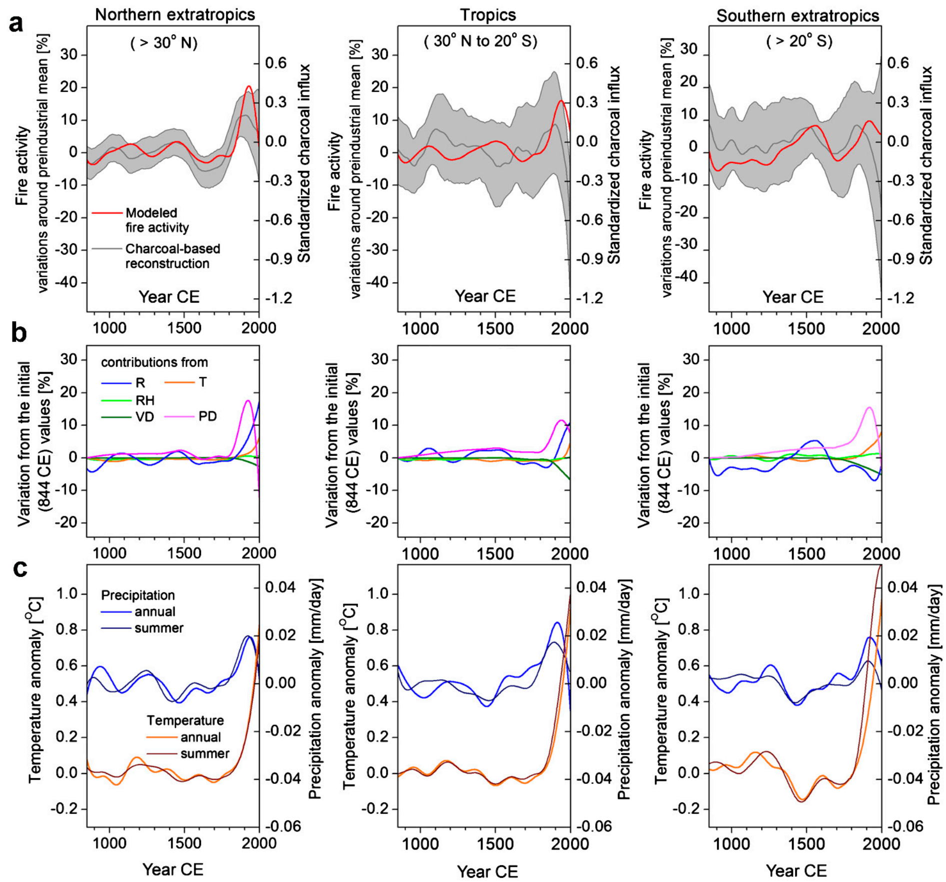

Fig. S4. Zonal fire activity trends. (*a*) Modeled variations of fire activity (red line) and charcoal-based reconstruction of fires (black line with gray-shaded confidence interval) (21) in the northern extratropical (>30 °N), tropical (30 °N to 20 °S), and southern extratropical (>20 °S) zones. (*b*) Contribution of individual parameters to the zonal fire trends: precipitation (blue line), temperature (orange line), relative humidity (green line), population (magenta line), and vegetation (olive green line) densities. (*c*) GISS GCM zonal annual and summer means of the terrestrial surface temperature (orange and wine lines), precipitation (light blue and navy lines).

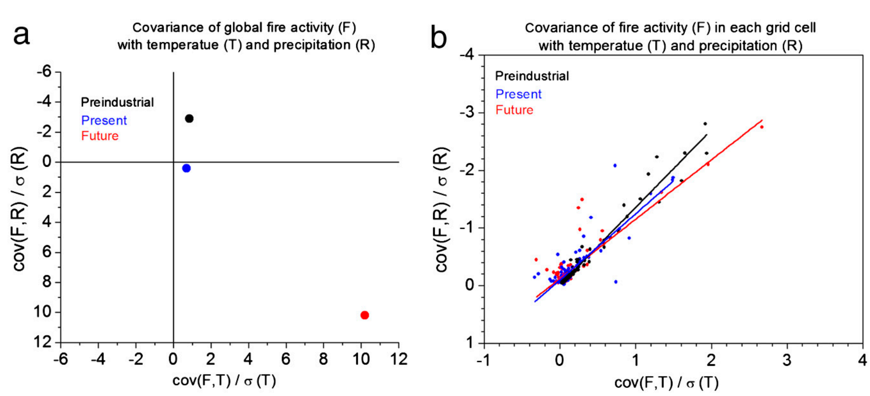

Fig. S5. Covariance of preindustrial (black), present (blue), and future (red) fire activity with temperature (x axis) and precipitation (y axis), normalized by temperature or precipitation variations (respectively). (*a*) Covariance of global average trends. (*b*) Covariance of variations in each grid cell normalized by temperature or precipitation variations in that cell. (Lines show linear fits to covariance at all cells during each time period.) Note that the y-axis scale is inverted (fire activity increases, as precipitation decreases).